Spectrochimica Acta Part A: Molecular and Biomolecular Spectroscopy 117 (2014) 1–8

Contents lists available at ScienceDirect

Spectrochimica Acta Part A: Molecular and Biomolecular Spectroscopy

journal homepage: www.elsevier.com/locate/saa

Mn(II) and Cu(II) complexes of a bidentate Schiff's base ligand: Spectral, thermal, molecular modelling and mycological studies

Monika Tyagi, Sulekh Chandra *, Prateek Tyagi

Department of Chemistry, Zakir Husain Delhi College, University of Delhi, JLN-Marg, New Delhi 110002, India

HIGHLIGHTS

- Synthesis and characterization of ligand by various spectral methods.
- Mn(II) and Cu(II) complexes were found to octahedral and tetragonal geometry, respectively.
- Thermal data suggested that complexes are more stable as compared to ligand.
- *In vitro* antifungal activity of synthesized compounds were screened against fungal species.
- All the complexes were found to be more active as compared to parent ligand.

GRAPHICAL ABSTRACT

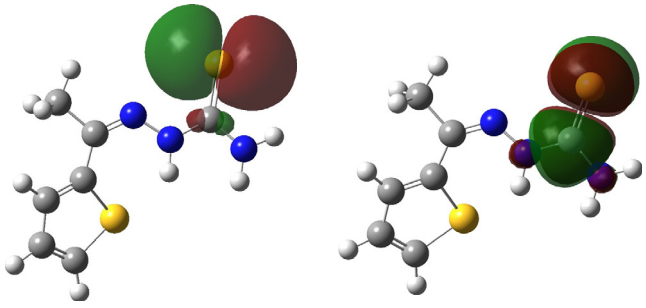

(a) (b)

ARTICLE INFO

Article history:
Received 17 April 2013
Received in revised form 3 July 2013
Accepted 21 July 2013
Available online 8 August 2013

Keywords:
Mn(II) and Cu(II) complexes
Thiosemicarbazone
Spectral characterization
Ths molecular modelling
Mycological studies

ABSTRACT

Complexes of manganese(II) and copper(II) of general composition $M(L)_2X_2$ have been synthesized [L = 2-acetyl thiophene thiosemicarbazone and X = Cl^- and NO_3^-]. The elemental analysis, molar conductance measurements, magnetic susceptibility measurements, mass, IR, UV, NMR and EPR spectral studies of the compounds led to the conclusion that the ligand acts as a bidentate manner. The Schiff's base ligand forms hexacoordinated complexes having octahedral geometry for Mn(II) and tetragonal geometry for Cu(II) complexes. The thermal studies suggested that the complexes are more stable as compared to ligand. In molecular modelling the geometries of Schiff's base and metal complexes were fully optimized with respect to the energy using the 6-31g(d,p) basis set. The mycological studies of the compounds were examined against the plant pathogenic fungi i.e. *Rhizoctonia bataticola*, *Macrophomina phaseolina*, *Fusarium odum*.

Introduction

The Schiff base contain azomethine group (—CH=N—). They are used as substrates in the preparation of industrial and biologically active compounds *via* ring closure, cycloaddition and replacement reactions [1]. Schiff's base ligands are potentially capable of forming stable complexes with most transition metal ions which served as model compounds for biologically important species [2]. Schiff base having thiosemicarbazide moiety can coordinate to metal as neutral molecules or after deprotonation as anionic ligands and can adopt variety different coordination modes. The possibility of their being able to transmit electronic effects between a reduce unit and metal centre is suggested by the delocalization of the bonds in the thiosemicarbazone chain [3]. Thiosemicarbazones and their metal complexes have considerable interest because of their biological activities, such as antitumour, antiviral, anticancer, antifungal, antibacterial and antimalarial [4–10]. They also have been used as drugs and are reported to possess a wide variety of biological activities against bacteria, fungi and certain type of tumors and also are useful model for bioinorganic processes

* Corresponding author. Tel.: +91 1122911267; fax: +91 1123215906.
E-mail addresses: mnk02tyg@yahoo.co.in (M. Tyagi), schandra_00@yahoo.com (S. Chandra).

1386-1425/$ - see front matter © 2013 Elsevier B.V. All rights reserved.
http://dx.doi.org/10.1016/j.saa.2013.07.074

[11,12]. Taking into consideration the above facts, Mn(II) and Cu(II) complexes of Schiff base derived from condensation of thiosemicarbzide and 2-acetyl thiophene were synthesized. The synthesized compounds were characterized using various spectral techniques and evaluated for their mycological studies against plant pathogenic fungi i.e. *Rhizoctonia bataticola*, *Macrophomina phaseolina*, *Fusarium odum*.

Experimental

Materials and methods

All the chemicals used were of Anala R grade and received from Sigma–Aldrich and Fluka. Metal salts were purchased from E. Merck and were used as received.

Synthesis of ligand

Hot ethanolic (20 mL) solution of thiosemicarbazide (0.91 g, 0.01 mol) and an ethanolic (20 mL) solution of 2-acetyl thiophene (1.26 g, 0.01 mol) were mixed. This mixture was refluxed at 70–80 °C for 2–3 h. On cooling the reaction mixture, white product was precipitated out. It was filtered off, washed with cold EtOH and dried under vacuum over P_4O_{10}. Yield 70%, mp 161 °C. Elemental analyses Found (Calcd.) for $C_7H_9N_3S_2$: C, 42.29 (42.21); H, 4.48 (4.52); N, 21.05 (21.10)%. Scheme of synthesis of ligand is given in Scheme 1.

Synthesis of metal complexes

Hot ethanolic solution (10 mL) of metal salt (nitrate or chloride) (1 mmol) were mixed with a hot ethanolic solution (15 mL) of the respective ligand (2 mmol). The reaction mixture was refluxed for 8–10 h at 80–85 °C. On keeping the resulting mixture overnight at 0 °C, the coloured product was separated out, which was filtered off, washed with cold ethanol and dried under *vacuum* over P_4O_{10}. The purity of the complexes was checked by TLC. TLC analysis was performed on silica gel using the solvent system benzene/acetone (1:2) as eluent.

Analysis

The carbon and hydrogen were analyzed on Carlo-Erba 1106 elemental analyzer. The nitrogen content of the complexes was determined using Kjeldahl's method. Molar conductance was measured on the ELICO (CM82T) conductivity bridge. Magnetic susceptibilities were measured at room temperature on a Gouy balance using $CuSO_4{\cdot}5H_2O$ as callibrant. Electronic impact mass spectrum was recorded on JEOL, JMS – DX-303 mass spectrometer. IR spectra (KBr) were recorded on FTIR spectrum BX-II spectrophotometer. NMR spectra were recorded with a model Bruker Advance DPX-300 spectrometer operating at 300 MHz using DMSO-d6 as a solvent and TMS as internal standard. The electronic spectra were recorded in DMSO on Shimadzu UV mini-1240 spectrophotometer. Thermogravimetric analysis (TGA and DTG) were carried out in dynamic nitrogen atmosphere (30 ml/min) with a heating rate of 10 C/min using a Schimadzu TGA-50H thermal analyzer. EPR spectra of the Mn(II) and Cu(II) complexes were recorded as polycrystalline sample at room temperature on E_{4-} EPR spectrometer using the DPPH as the g-marker.

Molecular modelling studies

The DFT calculations were performed using the B3LYP three parameter density functional, which includes Becke's gradient exchange correction [13], the Lee, Yang, Parr correlation functional [14] and the Vosko, Wilk, Nusair correlation functional [15]. The geometries of Schiff base and metal complexes were fully optimized with respect to the energy using the 6-31g(d,p) basis set using the Gaussian 09W suite [16].

Biological screening

The Poison food Technique [17,18] was employed to examine the synthesized compounds against the fungi, i.e. *R. bataticola*, *M. phaseolina* and *F. odum* for their fungicidal investigations. DMSO and Bavistin were employed as a control and a standard fungicide, respectively. The mycelial growth of fungi (mm) in each petriplate was measured diametrically and growth inhibition (*I*) was calculated using the formula: $I\,(\%) = (CT)/C \times 100$, where I = % Inhibition, C = Radial diameters of the colony in control, T = Radial diameter of the colony in test compound.

Results and discussion

The complexes were synthesized by reacting ligand with the metal ions in 2: 1 M ratio in ethanolic medium. On the basis of elemental analysis, the complexes were found to have the composition, as given in Table 1. The molar conductance of the complexes in DMSO lies in the range of 07–12 Ω^{-1} cm^2 mol^{-1} indicating their non-electrolytic behaviour [19]. Thus the complexes may be formulated as $[M(L)X_2]$ [where M = Mn(II), and Cu(II), X = Cl^-, NO_3^-].

Mass spectrum

The electronic impact mass spectrum of ligand showed a molecular ion peak at m/z = 200 amu corresponding to species $[C_7H_9N_3S_2]^-$ which confirms the proposed formula. It also shows series of peaks at 16, 60, 75, 101, 123, 132 and 184 amu corresponding to various fragments. The intensities of these peaks give the idea of the stabilities of the fragments (Supplementary material).

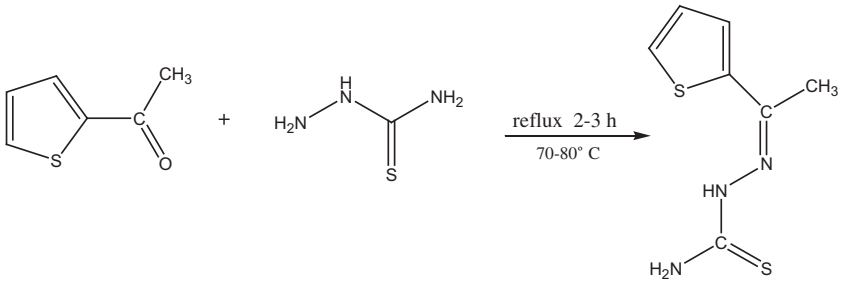

Scheme 1. Structure of ligand.

Table 1
Analytical data of Mn(II) and Cu(II) complexes.

Complexes	Colour	Yield (%)	M.p. (°C)	Elemental analysis found (calcd.) (%)				μ_{eff} BM
				M	C	H	N	
$[Mn(L)_2Cl_2]$	Off	59	178	10.42	32.00	3.00	16.08	5.92
$MnC_{14}H_{18}N_6S_4Cl_2$	White			(10.50)	(32.06)	(3.40)	(16.03)	
$[Mn(L)_2(NO_3)_2]$	Off	62	187	9.48	29.07	3.10	19.35	5.95
$MnC_{14}H_{18}N_8O_6S_4$	White			(9.53)	(29.12)	(3.12)	(19.41)	
$[Cu(L)_2Cl_2]$	Green	65	183	11.79	31.53	3.30	14.31	1.97
$CuC_{14}H_{18}N_6S_4Cl_2$				(11.84)	(31.58)	(3.38)	(14.36)	
$[Cu(L)_2(NO_3)_2]$	Green	68	192	10.74	28.67	3.02	19.00	1.94
$CuC_{14}H_{18}N_8O_6S_4$				(10.77)	(28.72)	(3.07)	(19.14)	

^{1}H NMR spectrum

^{1}H NMR spectrum of ligand (Supplementary material) in DMSO exhibit following signals: δ 8.76 ppm (s) (1H, HN-CS), δ 6.42 ppm (s) (2H, H_2N—), δ 2.3 ppm (s) (3H, CH_3) and δ 7.1–7.3 ppm (m) (3H, thiophene ring).

IR spectra

The important IR bands of the compounds along with their assignments are given in Table 2. In principle, the ligand can exhibit thione-thiol tautomerism since it contains a thioamide—NH—C=S functional group. The ν(S—H) band at 2565 cm^{-1} is absent in the IR spectrum of ligand but ν(N—H) band at 3205 cm^{-1} is present, indicating that in the solid state, the ligand remains as the thione tautomer. The position of ν(C=N) band of the thiosemicarbazone appeared at 1592 cm^{-1} is shifted towards lower side in the complexes indicating coordination via the azomethine nitrogen [20,21]. This is also confirmed by the appearance of new band in complexes in the range of 450–475 cm^{-1}, which has been assigned to the ν(M—N) [22]. In the IR spectrum of ligand the band appeared at 756 cm^1 corresponding to ν(C=S) is shifted towards lower side. It indicates that thione sulphur coordinates to the metal ion [23]. Thus, it may be concluded that behaves as bidentate chelating agent coordinating through azomethine nitrogen and thiolate sulphur. The presence of bands at 1450–1410 (ν_5), 1348–1320 (ν_1) and 1058–1025 (ν_2) cm^{-1}, in the IR spectra of the metal complexes suggest that both the nitrate groups are coordinated to the central metal ion in a unidentate fashion [24].

Magnetic moments

The magnetic moment observed for Mn(II) complexes lies in the range 5.92–5.95 BM corresponding to five unpaired electrons. At room temperature Cu(II) complexes show magnetic moment in the range 1.94–1.97 BM corresponding to one unpaired electron [25]. The observed magnetic moments of Mn(II) and Cu(II) complexes are given in Table 1.

Electronic spectra

Electronic spectra of Mn(II) complexes exhibit four weak intensity absorption bands in the range 18,182–18,349, 22,883–24,630, 26,880–28,736 and 31,250–35,087 cm^{-1}. These bands may be assigned to the $^6A_{1g} \rightarrow {}^4T_{1g}(^4G)$, $^6A_{1g} \rightarrow {}^4E_g$, $^4A_{1g}$ (^4G) (10B + 5C) and $^6A_{1g} \rightarrow {}^4E_g$ (^4D) (17B + 5C) and $^6A_{1g} \rightarrow {}^4T_{1g}(^4P)$ transitions, respectively, corresponding to an octahedral geometry [26]. Electronic spectra of Cu(II) complexes show the d–d transition bands in the range 12,188–15,479, 18,621–19,132 and 24,402–27,322 cm^{-1}. These bands correspond to $^2B_{1g} \rightarrow {}^2A1g$ ($d_{x2-y2} \rightarrow d_{z2}$) ν_1, $^2B1g \rightarrow {}^2B_{2g}$ ($d_{x2-y2} \rightarrow d_{xy}$) ν_2 and $^2B_{1g} \rightarrow {}^2E_g$ ($d_{x2-y2} \rightarrow d_{xz}$, d_{yz}) ν_3 and transitions, respectively [27]. An elongated tetragonal geometry has been assigned for Cu(II) complex. The spectra of all the complexes have been vibronically assigned to D_{4h} symmetry with a d_{x2-y2} ground state.

Electronic paramagnetic resonance spectra

EPR spectra of Mn(II) complexes were recorded at room temperature as polycrystalline samples and in DMSO solution. The polycrystalline spectra give an isotropic signal centered at 1.95–2.06. In DMSO solution the complexes give well resolved six lines due to hyperfine interaction between the unpaired electrons with the ^{55}Mn nucleus (I = 5/2). EPR spectra of the Cu(II) complexes were recorded, at room temperature as polycrystalline samples, on the X-band at 9.1 GHz under the magnetic field range 3000G. The analysis of spectra of Cu(II) complexes (Supplementary material) give g 2.12–2.21 and g 2.08–2.16. The trend $g > g > 2.0023$, observed for the complexes, under study, indicate that the unpaired electron is localized in the d_{x2-y2} orbital of the Cu(II) ion and the spectral figures are characteristic for the axial symmetry. Tetragonally elongated geometry is thus confirmed for the afore-said complexes [28]. $G = (g - 2)/(g - 2)$, which measure the exchange interaction between the metal centres in a polycrystalline solid has been calculated. According to Hathaway and Billing [29] if $G > 4$ the exchange interaction is negligible, but G indicates considerable exchange interaction in the solid complexes. The complexes reported in this paper gives the 'G' value (Table 3) in the range 1.31–1.44, which is <4, indicating exchange interaction in the solid complexes.

Thermal analysis

Schiff's base and its metal lexes were studied by thermogravimetric analysis from ambient temperature to 800 °C in nitrogen atmosphere. The TG curves were redrawn as % mass loss vs.

Table 2
Important infrared spectral (cm^{-1}) bands and their assignments.

Compounds	Assignments				Bands due to anions
	ν(N—H)	ν(C=N)	ν(M—N)	ν(M—S)	
$[Mn(L)_2Cl_2]$	3150	1570	462	318	
$[Mn(L)_2(NO_3)_2]$	3195	1582	450	305	ν_5 = 1450, ν_1 = 1348, ν_2 = 1058 $\Delta(\nu_5-\nu_1)$ = 102 cm^{-1} indicating unidentate nature
$[Cu(L)_2Cl_2]$	3165	1565	475	322	
$[Cu(L)_2(NO_3)_2]$	3240	1576	470	312	ν_5 = 1410, ν_1 = 1320, ν_2 = 1025 $\Delta(\nu_5-\nu_1)$ = 90 cm^{-1} indicating unidentate nature

Table 3
Electronic spectral bands (cm^{-1}) and EPR spectral data of the complexes.

Compounds	λ_{max} (cm^{-1})	g	g	g_{iso}	G
$[Mn(L)_2Cl_2]$	18,182, 22,883, 26,880, 31,250	–	–	1.95	–
$[Mn(L)_2(NO_3)_2]$	18,349, 24,630, 28,736, 35,087	–	–	2.06	–
$[Cu(L)_2Cl_2]$	12,188, 18,621, 24,402	2.12	2.08	2.10	1.44
$[Cu(L)_2(NO_3)_2]$	15,479, 19,132, 27,322	2.21	2.16	2.17	1.31

temperature (TG) curves. Typical TG curves are presented in Fig. 1 and the temperature ranges and percentage mass losses of the decomposition reaction are given in Table 4 together with evolved moiety and the theoretical percentage mass losses thermal techniques, such as thermogravimetric analysis (TGA and DTG), has been successfully employed for the study of the energetic of interactions of metal cations with biological species, such as amino acids [30,31]. The weight loss profiles are analyzed the amount or percent of weight loss at any given temperature, and the temperature ranges of the degradation process were determined. Thermal stability domains, melting points, decomposition phenomena and their assignments for the Schiff, s base and its complexes are

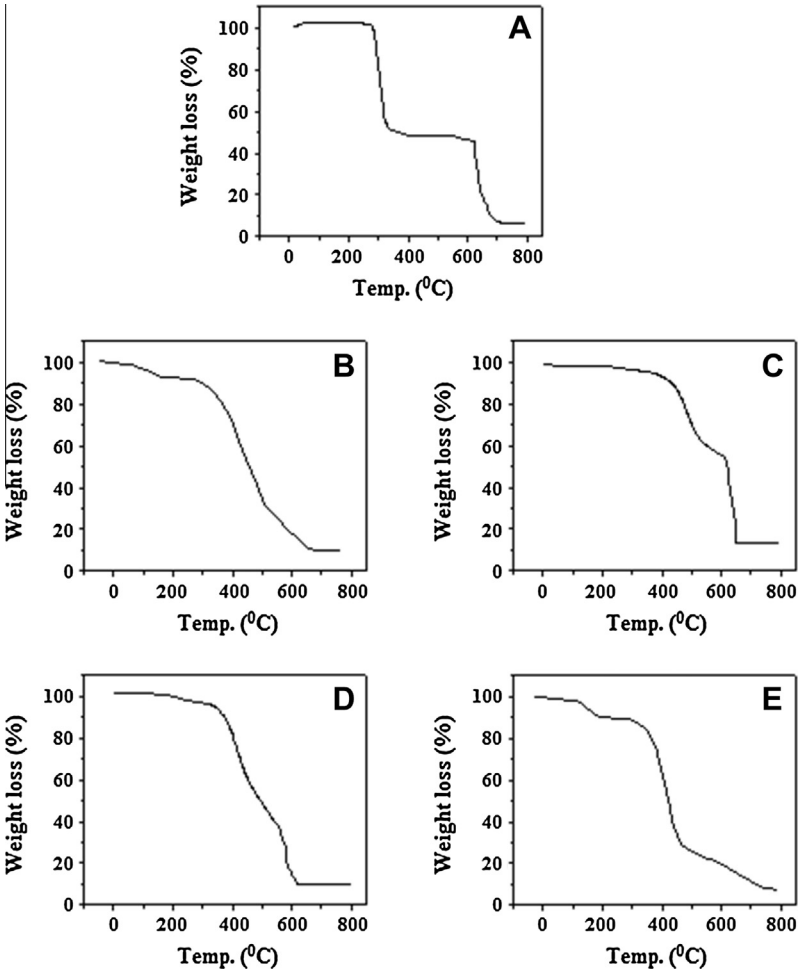

Fig. 1. TGA curves of (A) ligand (L), (B) $[Mn(L)_2Cl_2]$, (C) $[Mn(L)_2(NO_3)_2]$, (D) $[Cu(L)_2Cl_2]$, and (E) $[Cu(L)_2(NO_3)_2]$ complexes in nitrogen atmosphere.

Table 4
Thermoanalytical results (TG and DTG) for the Schiff's base and its complexes.

Complexes	Stages	Temp. (K)	DTG $_{max}$ (°C)	Residual species	Decomposition species	Total losses (%)	
						Found	Calc.
$C_7H_9N_3S_2$ (L)	Ist 2nd	120–400 400–800	320	–	—$C_3H_5N_3S$(organic moiety) C_4H_4S (thiophene ring)	99.9	100
$[Mn(L)_2Cl_2]$ $MnC_{14}H_{18}N_6S_4Cl_2$	Ist 2nd	120–300 300–800	280 435	MnS	—H_4N_2(hydrazine molecule) $C_{14}H_{14}N_4S_3Cl_2$(organic moiety)	83.4	83.8
$[Mn(L)_2(NO_3)_2]$ $MnC_{14}H_{18}N_8O_6S_4$	Ist 2nd	120–420 420–800	290 475	MnO_2	—$C_2H_4N_2O_2$(2amido group) —$C_{12}H_{14}N_6O_2S_4$(organic moiety)	84.9	84.5
$[Cu(L)_2Cl_2]$ $CuC_{14}H_{18}N_6S_4Cl_2$	Ist 2nd	120–280 280–800	185 452	CuS	—H_4N_2(hydrazine molecule) $C_{14}H_{14}N_4S_3Cl_2$(organic moiety)	82.1	82.1
$[Cu(L)_2(NO_3)_2]$ $CuC_{14}H_{18}N_8O_6S_4$	Ist 2nd	120–200 200–800	180 432	CuO	$C_2H_4N_2O_2$(2amido group) $C_{12}H_{14}N_6O_3S_4$(organic moiety)	86.4	86.6

Table 5
Optimized geometry of the ligand and metal complexes (bond lengths in Angstroms; bond angles in degrees).

Parameters[a]	Ligand (L)	$[M(L_2)XX']$[b]	$[M(L_2)XX']$[c]	$[M(L_2)XX']$[d]	$[M(L_2)XX']$[e]
M—X	–	2.491	2.093	2.526	2.030
M—X′	–	2.426	1.969	2.367	1.979
M—S_1	–	2.639	2.620	4.650	3.964
M—N_2	–	2.000	2.013	2.006	2.006
M—S_3	–	2.524	2.542	2.654	2.618
M—N_4	–	2.076	2.033	2.041	2.023
S_1—C_1	1.713	1.732	1.741	1.719	1.722
C_1—N_3	1.365	1.348	1.344	1.361	1.355
C_1—N_1	1.382	1.358	1.366	1.384	1.386
N_1—N_2	1.370	1.429	1.442	1.413	1.424
N_2—C_2	1.305	1.332	1.320	1.317	1.316
S_3—C_8	–	1.733	1.745	1.728	1.739
C_8—N_6	–	1.352	1.349	1.357	1.352
C_8—N_5	–	1.350	1.347	1.360	1.356
N_4—N_5	–	1.407	1.410	1.392	1.382
N_4—C_9	–	1.317	1.318	1.313	1.308
S_1MN_2	–	78.42	77.32	33.92	51.32
S_3MN_4	–	81.92	81.99	82.53	82.87
S_1MX_1	–	87.04	84.94	95.04	79.34
N_2MX_2	–	95.12	89.08	96.36	90.7
N_4MX_1	–	84.28	85.62	82.15	85.16
S_3MX_2	–	94.60	99.25	110.32	113.53
X_1MX_2	–	174.95	176.23	146.84	144.44

L = 2-acetyl thiophene thiosemicarbazone.
[a] See Scheme 1 for numbering.
[b] M = Mn, X = Cl and X′ = Cl′.
[c] M = Mn, X = NO_3 and X′ = NO_3'.
[d] M = Cu, X = Cl and X′ = Cl′.
[e] M = Cu, X = NO_3 and X′ = NO_3'.

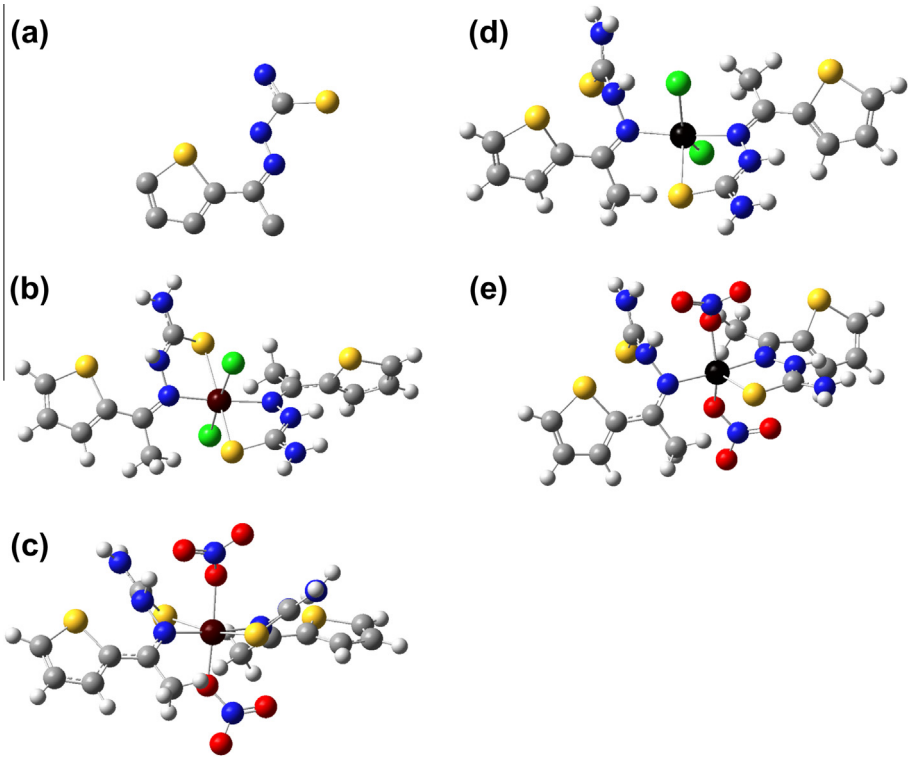

Fig. 2. Geometry optimized structure of (a) Schiff base, (b) $[Mn(L)_2Cl_2]$, (c) $[Mn(L)_2(NO_3)_2]$, (d) $[Cu(L)_2Cl_2]$, (e) $[Cu(L)_2(NO_3)_2]$ (colour code: H-White, C-Grey, N-Blue, O-Red, Mn = Brown, Cu-Black). (For interpretation of the references to colour in this figure legend, the reader is referred to the web version of this article.)

summarized in Table 4. The overall loss of mass from the TG curves is 83.40% for $[Mn(L)_2Cl_2]$, 84.92 for $[Mn(L)_2(NO_3)_2]$ 82.14% for $[Cu(L)_2Cl_2]$ and 86.49% for $[Cu(L)_2(NO_3)_2]$. All the complexes show two essential maxima peaks corresponding to mass loss. The first sharp endothermic peak corresponding to complexes of $[Mn(L)_2Cl_2]$ and $[Cu(L)_2Cl_2]$ occurring between 120 and 300 °C may be due to loss of hydrazine molecule (N_2H_4) and the second decomposition step in the range of 280–800 °C, correspond to the pyrolysis of organic moiety. In nitrato complexes of Mn(II) and Cu(II) the first sharp endothermic peak observed between 120 and 420 °C may be

Table 6
Fungicidal screening data of compounds showing growth inhibition (%) at 250, 500 and 750 ppm concentrations after 7 days at 26 ± 1 °C.

Compounds	*R. bataticola*			*M. phaseolina*			*F. odum*		
	250	500	750	250	500	750	250	500	750
Ligand (L)	25	35	44	42	54	63	32	44	56
[Mn(L)2Cl2]	48	50	65	52	52	71	53	64	74
$[Mn(L)_2(NO_3)_2]$	50	59	68	57	68	80	42	53	65
[Cu(L)2Cl2]	81	90	98	75	91	100	59	71	89
$[Cu(L)_2(NO_3)_2]$	70	79	85	70	87	92	68	76	94
Chlorothalonil	86	91	100	68	78	90	70	82	98
DMSO	0	0	0	0	0	0	0	0	0

due to loss of amido group and the second decomposition step corresponding to the pyrolysis of organic moiety.

Molecular modelling analysis

Geometry Optimization was done using B3LYP functional with 6-31G(d,p) basis sets as incorporated in the Gaussian 09W programme in gas phase. $[Mn(L)_2Cl_2]$ and $[Mn(L)_2(NO_3)_2]$ complexes have octahedral geometry with slight distortion. The two axial positions are occupied by chloride ions/oxygen of nitrate ions respectively, while the equatorial positions are being occupied by nitrogen and sulphur atoms of the ligand. The two equatorial Mn—S distances are 2.639 Å and 2.524 Å in $[Mn(L)_2Cl_2]$ complex while 2.620 Å and 2.542 Å in $[Mn(L)_2(NO_3)_2]$ complex. The Mn—N bond distances are 2.000 Å and 2.076 Å in $[Mn(L)_2Cl_2]$ complex while 2.013 Å and 2.033 Å respectively in $[Mn(L)_2(NO_3)_2]$ complex. The axial Mn—Cl bond distances in $[Mn(L)_2Cl_2]$ complex are 2.491 Å and 2.426 Å respectively. Similarly the axial Mn—O bond distances in $[Mn(L)_2(NO_3)_2]$ complex are 2.093 Å and 1.969 Å. The bond angles in the coordination sphere of Mn(II) complexes are found approximately near to the perpendicular value. The S_1—Mn—N_2, S_1—Mn—Cl_1, S_3—Mn—Cl_2 and N_2—Mn—Cl_2 bond angles are 78.42°, 87.04°, 94.60° and 95.12° respectively. The bond angle Cl_1—Mn—Cl_2 is found to be 174.95°. Similar results are obtained in case of $[Cu(L)_2Cl_2]$ and $[Cu(L)_2(NO_3)_2]$ complexes, all the bond lengths except Cu—S_1 bond have very close value to as compared to Mn(II) complexes. The Cu—S_1 bond lengthens to 4.65 Å in $[Cu(L)_2Cl_2]$ complex and 3.96 Å in $Cu(NO_3)_2$ complex, which results in strong distortion from regular octahedral geometry. It is due to distortion that bond angle S_1—Cu—N_2 reduces to 33.92° in $[Cu(L)_2Cl_2]$ complex and 51.92° in $[Cu(L)_2(NO_3)_2]$. The calculated bond length and bond angle for the ligand and their metal complexes

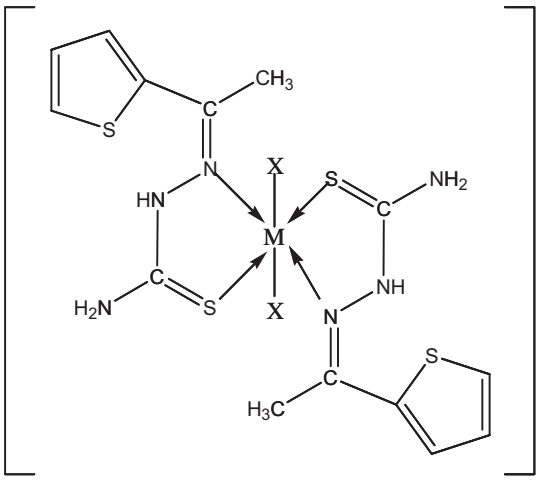

Where X= Cl^-, NO_3^- and M= Mn(II) , Cu(II)

Fig. 4. Suggested structure of Mn(II) and Cu(II) complexes.

are listed in Table 5. The optimized structure of Schiff base and metal complexes are given in Fig. 2.

Mulliken population analysis method is used to determine the Mulliken charges on ligand atoms and metal complexes. The computed charges are given in Table 6. The charge of the Mn^{2+} ion in the Free State is +2.0. It is seen that the positive charge of the metal ion decreases to +0.810 in $[Mn(L)_2Cl_2]$ complex, which indicates that transfer of electrons from the ligands to the metal ion has occurred and the coordination bonds have formed. To see how the charge transfer occurs, we compared the values of partial atomic charges on the free ligand with that of the $Mn(L)_2Cl_2$ complex, in which the charge transfer takes place.

According to Pearson's HSAB concept, Mn^{2+} is a hard acid and Cl^{1-} is a hard base, while S^{2-} is a soft base and N^{3-} comes in borderline. This indicates that there should be a stronger interaction between Mn^{2+} & Cl^{1-} than between Mn^{2+} & N^{3-} and Mn^{2+} & S^{2-} respectively. Our calculations are in accord with this principle, as there is a transfer of $^-0.862e$ from two chloride ions and $^-0.328e$ are transferred from the rest if the ligand to Manganese metal. This shows that a total of ~1.119*e* is transferred to Mn(II) during the complexation, and the net charge on the Mn(II) reduces to ~0.810*e*. Similar behaviour in charge transfer is noted in case of $[Mn(L)_2(NO_3)_2]$, $[Cu(L)_2Cl_2]$ and $[Cu(L)_2(NO_3)_2]$ complexes. The

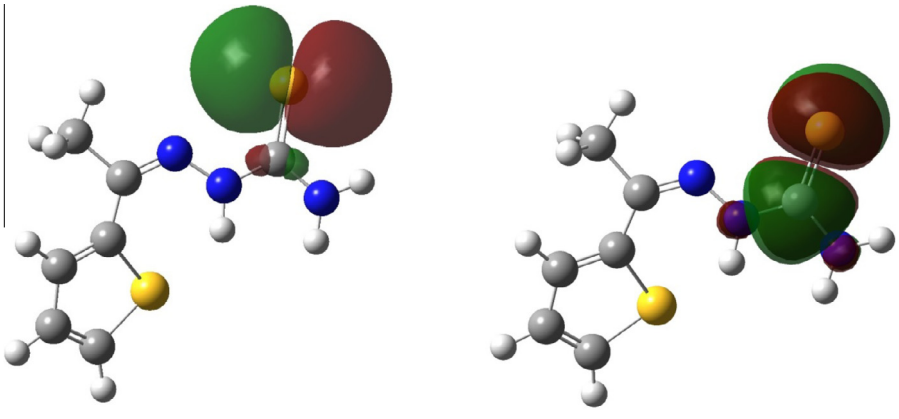

Fig. 3. Plot of HOMO and LUMO of 2-acetyl thiophene thiosemicarbazone.

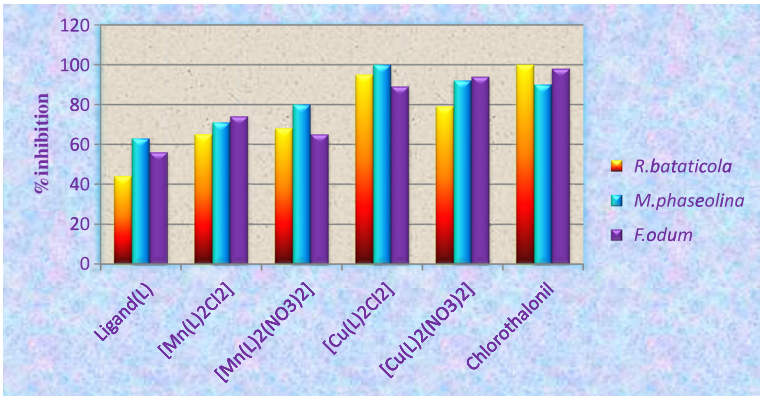

Fig. 5. Graph showing the inhibition percentage of synthesized compounds against fungus species.

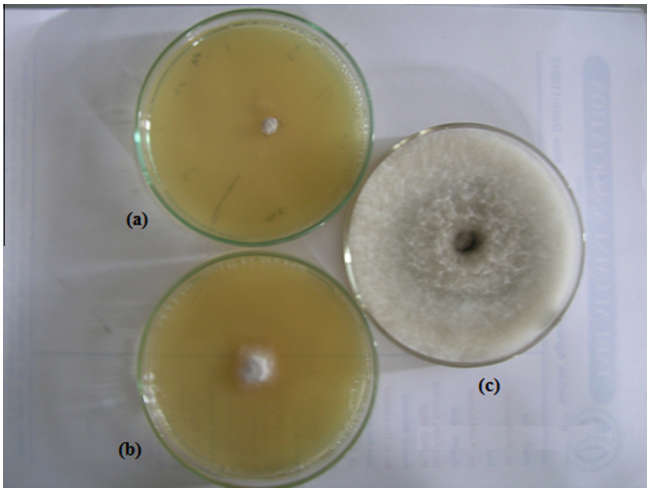

Fig. 6. Comparison of the growth of $[Cu(L)Cl_2]$ complex against fungus *Rhizoctonia bataticola* (a) at 750 ppm, (b) 500 ppm, and (c) control plate.

charge on central metal ion after complexation reduces to 1.104*e*, 0.716*e* and 0.967*e* respectively.

A noteworthy point is the similarity in trend of charge transfer in Mn(II) and Cu(II) complexes, as chloride ions acts as a better electron donor than nitrate ion. There is a transfer of 0.862*e* from chloride ion in $[Mn(L)_2Cl_2]$ complex and 0.911*e* are donated by chloride ion in $Cu(L)_2Cl_2$ complex during complex formation, while in case of nitrate ion there is a transfer of only 0.575*e* and 0.623*e* in $[Mn(L)_2(NO_3)_2]$ complex and $[Cu(L)_2(NO_3)_2]$ respectively.

We also calculated the energies for Highest occupied molecular orbital (HOMO) and Lowest occupied molecular orbital (LUMO). The calculated energies of the HOMO and LUMO for ligand are −0.183 hartree and −0.081 hartree, respectively. The HOMO of the ligand is concentrated on S_1 atom, while LUMO is concentrated on S_1 and C_1 atoms. The 0.020 hartree isovalue contours for the HOMO and LUMO are displayed in Fig. 3.

On the basis of above discussion following (Fig. 4) can be proposed for the synthesized complexes (see Fig. 4).

Antimicrobial studies

The antimicrobial screening data show that the compounds exhibit antimicrobial properties and it is important to note that the metal chelates exhibit more inhibitory effects than the parent ligands (Fig. 5). The increased activity of metal complexes can be explained on the basis of chelation theory [32]. It has also been proposed that concentration plays a vital role in increasing the degree of inhibition; as the concentration increases (Fig. 6) the activity increases (Table 6).

The activity order for *R. bataticola* was found to be

Chlorothalonil > $[Cu(L)_2Cl_2]$ > $[Cu(L)_2(NO_3)_2]$ > $[Mn(L)_2Cl_2]$ > $[Mn(L)_2(NO_3)_2]$ > Ligand

With *M. phaseolina* the order of activity was

$[Cu(L)_2Cl_2]$ > $[Cu(L)_2(NO_3)_2]$ > Chlorothalonil > $[Mn(L)_2(NO_3)_2]$ > $[Mn(L)_2Cl_2]$ > Ligand

The order of activity with *F. odum* was found to be:

Chlorothalonil > $[Cu(L)_2(NO_3)_2]$ > $[Cu(L)_2Cl_2]$ > $[Mn(L)_2Cl_2]$ > $[Mn(L)_2(NO_3)_2]$ > Ligand.

Conclusion

The thiosemicarbazide based Schiff's base has been synthesized and its coordination behaviour with Mn(II) and Cu(II) metal ions has also been studied. On the basis of spectral studies Mn(II) complexes were found to have an octahedral geometry whereas the Cu(II) complexes have tetragonal geometry. The thermal studies suggested that the complexes are more stable as compared to ligand. Molecular modelling calculations results hold a good comparison between the theoretically predicted geometries and the experimental ones, which is clearly validating our methodology. Although these calculations pertain to the gas phase, and the experimental data are for the solid state, in which crystal field effect may affect the relative energies and geometries. In the biological environment, hydrogen bonding with the solvent is also expected to affect the relative energies and geometries, but the good correspondence between our calculations and experimental data suggest that crystal packing and hydrogen bonding effects are negligible. The fungicidal screening of the compounds led to the conclusion that metal complexes are more active as compared to free ligand.

Acknowledgements

We thank the Principal, Zakir Husain Delhi College for providing lab facilities, IIT Bombay for recording EPR spectra, IIT delhi for recording NMR spectra. Authors are thankful to UGC, New Delhi for financial assistance.

Appendix A. Supplementary material

Supplementary data associated with this article can be found, in the online version, at http://dx.doi.org/10.1016/j.saa.2013.07.074.

References

[1] C.R. Choudhary, S.K. Mondal, S. Mitra, S.D.G. Mahali, K.M.A. Malik, J. Chem. Crystallogr. 31 (2002) 57.
[2] F.R. Pavan, P.I. da, S. Maia, S.R.A. Leite, V.M. Deflon, A.A. Batista, D.N. Sato, S.G. Franzblau, C.Q.F. Leite, Eur. J. Med. Chem. 45 (2010) 1898.
[3] S. Tardito, L. Marchiò, Curr. Med. Chem. 16 (2009) 1325.
[4] M.B. Ferrari, F. Bisceglie, A. Buschini, S. Franzoni, G. Pelosi, S. Pinelli, P. Tarasconi, M. Tavone, J. Inorg. Biochem. 104 (2010) 199.
[5] M.A. Neelakantan, M. Esakkiammal, S.S. Mariappan, J. Dharmaraja, T. Indian, J. Pharm. Sci. 72 (2010) 216.
[6] T.S. Lobana, R. Sharma, G. Bawa, S. Khanna, Coord. Chem. Rev. 253 (2009) 977.
[7] A.G. Quiroga, C.N. Ranninger, Coord. Chem. Rev. 248 (2004) 119.
[8] A. Corona-Bustamante, J.M. Viveros-Paredes, A. Flores-Parra, et al., Molecules 15 (2010) 5445.
[9] N. Raja, R. Ramesh, Spectrochim. Acta A 75 (2010) 713.
[10] S.A. Patil, V.H. Naik, A.D. Kulkarni, P.S. Badami, Spectrochim. Acta A 75 (2010) 347.
[11] M. Joseph, A. Sreekanth, V. Suni, M.R.P. Kurup, Spectrochim. Acta A 64 (2006) 637.
[12] G. Ibrahim, G. Bouet, I.H. Hall, M.A. Khan, J. Inorg. Biochem. 81 (2000) 29.
[13] M A.D. Becke, Phys. Rev. A 38 (1988) 3098.
[14] C. Lee, W. Yang, R.G. Parr, Phys. Rev. B 37 (1988) 785.
[15] S.H. Vosko, L. Wilk, M. Nusair, Can. J. Chem. 58 (1980) 1200.
[16] M.J. Frisch, G.W. Trucks, H.B. Schlegel, G.E. Scuseria, M.A. Robb, J.R. Cheeseman, G. Scalmani, V. Barone, B. Mennucci, G.A. Petersson, H. Nakatsuji, M. Caricato, X. Li, H.P. Hratchian, A.F. Izmaylov, J. Bloino, G. Zheng, J.L. Sonnenberg, M. Hada, M. Ehara, K. Toyota, R. Fukuda, J. Hasegawa, M. Ishida, T. Nakajima, Y. Honda, O. Kitao, H. Nakai, T. Vreven, J.A. Montgomery, Jr., J.E. Peralta, F. Ogliaro, M. Bearpark, J.J. Heyd, E. Brothers, K.N. Kudin, V.N. Staroverov, R. Kobayashi, J. Normand, K. Raghavachari, A. Rendell, J.C. Burant, S.S. Iyengar, J. Tomasi, M. Cossi, N. Rega, J.M. Millam, M. Klene, J.E. Knox, J.B. Cross, V. Bakken, C. Adamo, J. Jaramillo, R. Gomperts, R.E. Stratmann, O. Yazyev, A.J. Austin, R. Cammi, C. Pomelli, J.W. Ochterski, R.L. Martin, K. Morokuma, V.G. Zakrzewski, G.A. Voth, P. Salvador, J.J. Dannenberg, S. Dapprich, A.D. Daniels, O. Farkas, J.B. Foresman, J.V. Ortiz, J. Cioslowski, D.J. Fox, Gaussian, Inc., Wallingford CT, 2009.
[17] A.E. Liberta, D.X. West, Biometals 5 (1991) 121.
[18] M. Tyagi, S. Chandra, OJIC 2 (2012) 41.
[19] S. Chandra, S. Raizada, M. Tyagi, P. Sharma, Spectrochim. Acta A 69 (2008) 816.
[20] K.P. Deepa, K.K. Aravindakshan, Synth. React. Inorg. Met. Org. Chem. 30 (2000) 1601.
[21] N.S. Youssef, K.H. Hegab, Synth. React. Inorg. Met.-Org.Chem. 35 (2005) 391.
[22] S. Chandra, M. Tyagi, J. Serb. Chem. Soc. 73 (2008) 727.
[23] S. Chandra, L.K. Gupta, S. Agrawal, Trans. Met. Chem. 32 (2007) 240.
[24] S. Chandra, A.K. Sharma, Spectrochim. Acta A 74 (2009) 271.
[25] U. Kumar, S. Chandra, E – J. Chem. 7 (2010) 1238.
[26] M. Tyagi, S. Chandra, J. Indian Chem. Soc. 89 (2012) 147.
[27] A.B.P. Lever, Crystal field spectra, in: Inorganic Electronic Spectroscopy, first ed., Elsevier, Amsterdam, 1968.
[28] S. Chandra, U. Kumar, Spectrochim. Acta A 61 (2005) 219.
[29] B.J. Hathaway, D.E. Billing, Coord. Chem. Rev. 5 (1970) 143.
[30] S. Chandra, M. Tyagi, M.S. Refat, J. Serb. Chem. Soc. 74 (2009) 907.
[31] M.S. Refat, S. Chandra, M. Tyagi, J. Therm. Anal. Calorim. 100 (2010) 261.
[32] S. Chandra, A. Kumar, Spectrochim. Acta A 68 (2007) 1410.